Cell Tissue Res (1990) 260:495–505

Cell and Tissue Research

Organization of a phyllobranchiate gill from the green shore crab *Carcinus maenas* (Crustacea, Decapoda)

Saul H. Goodman and Michael J. Cavey

Division of Zoology, Department of Biological Sciences, The University of Calgary, Calgary, Alberta, Canada

Accepted September 20, 1989

Summary. The phyllobranchiate gills of the green shore crab *Carcinus maenas* have been examined histologically and ultrastructurally. Each gill lamella is bounded by a chitinous cuticle. The apical surface of the branchial epithelium contacts this cuticle, and a basal lamina segregates the epithelium from an intralamellar hemocoel. In animals acclimated to normal sea water, five epithelial cell types can be identified in the lamellae of the posterior gills: chief cells, striated cells, pillar cells, nephrocytes, and glycocytes. Chief cells are the predominant cells in the branchial epithelium. They are squamous or low cuboidal and likely play a role in respiration. Striated cells, which are probably involved in ionoregulation, are also squamous or low cuboidal. Basal folds of the striated cells contain mitochondria and interdigitate with the bodies and processes of adjacent cells. Pillar cells span the hemocoel to link the proximal and distal sides of a lamella. Nephrocytes are large, spherical cells with voluminous vacuoles. They are rimmed by foot processes or pedicels and frequently associate with the pillar cells. Glycocytes are pleomorphic cells packed with glycogen granules and multigranular rosettes. The glycocytes often mingle with the nephrocytes. Inclusion of the nephrocytes and glycocytes as members of the branchial epithelium is justified by their participation in intercellular junctions and their position internal to the epithelial basal lamina.

Key words: Cuticle – Epithelium, branchial – Gills – Hemocoel – Histology – Ultrastructure – *Carcinus maenas* (Crustacea)

The green shore crab *Carcinus maenas* is a euryhaline species, and its phyllobranchiate gills have garnered considerable attention owing to their involvement in respiration, ionoregulation, and excretion. While our physiological appreciation of the gills has been improving steadily, there is only fragmentary information on branchial histology and ultrastructure (Zatta and Milanesi 1984; Gilles and Péqueux 1985; Towle and Kays 1986).

Crustacean gills generally exhibit an adcuticular epithelium with circumscribed areas for gaseous exchange and salt transport. The salt-transporting areas tend to be restricted to the posterior gills of decapod crustaceans (Copeland 1968; Copeland and Fitzjarrell 1968; Barra et al. 1983; Gilles and Péqueux 1985). In preparation for experimental studies on the gills of *C. maenas*, we have surveyed the cuticle, the branchial epithelium, and the hemocoel. This report covers the gross morphology of a posterior gill, the histology of the branchial lamellae, and the ultrastructure of the lamellar components. It provides a preliminary description of cuspidate projections, tentatively called gill spines, over the excurrent hemolymph channel and illustrates a rich bacterial fauna that largely obscures the cuticular surface. Portions of this study have been published in abstract (Cavey and Curtis 1987; Goodman and Cavey 1988).

Materials and methods

Specimens

Adult crabs (*Carcinus maenas* L.) were obtained from the Marine Biological Laboratory (Woods Hole, MA, USA). They were maintained in refrigerated aquaria and acclimated to normal artificial sea water with a specific gravity of 1.025.

Light- and transmission electron microscopy

After removal of the carapace, the gills were flooded in situ with a primary fixative consisting of 2.5% glutaraldehyde, 0.2 M Millonig's phosphate buffer (pH 7.4), and 0.14 M sodium chloride (Cloney and Florey 1968). Whole gills, freed by cutting their attachments with iridectomy scissors, were placed in containers of primary fixative and sliced into multilamellar segments with razor blades.

Send offprint requests to: Dr. Michael J. Cavey, Department of Biological Sciences, The University of Calgary, 2500 University Drive N.W., Calgary, Alberta, Canada T2N 1N4

This operation frequently yielded individual lamellae (gill plates) as well. Elapsed time in the primary fixative was 1 h at ambient temperature. The specimens were immersed, without rinsing, in a secondary fixative consisting of 2% osmium tetroxide and 1.25% sodium bicarbonate buffer (pH 7.2) for 1 h at 4° C (Wood and Luft 1965). The gill plates and segments were then rinsed briefly with deionized water, dehydrated in graded solutions of ethanol, and exposed to propylene oxide. Rinsing, dehydration, and clearing were accomplished at ambient temperature.

The gill plates, owing to chitinous cuticles, were especially difficult to infiltrate. To overcome this problem, the specimens were gradually infiltrated with graded mixtures of propylene oxide and Epon (Luft 1961) for 4–8 h on the inclined table of a rotating mixer and in pure Epon for 14 h under vacuum (30–35 kPa). The specimens were subsequently transferred to pure epoxy resin in silicone rubber molds and carefully oriented. The molds were returned to the vacuum chamber for an additional 4 h and then placed in an oven at 60° C for 18 h.

Multilamellar segments and individual plates from the seventh gills were mounted on aluminum chucks, sectioned with glass knives on a Sorvall MT-2B ultramicrotome at a thickness of 1 μm, and stained on a laboratory hotplate with an alkaline solution of azure II and methylene blue (Richardson et al. 1960). These thin sections were viewed with a Nikon Alphaphot compound microscope equipped with planachromatic objective lenses and photographed with a Nikon Microflex AFX-II camera attachment.

Ultrathin sections (approximately 70 nm in thickness) were cut with diamond knives on a Sorvall MT-6000 ultramicrotome. The sections were collected on naked copper grids and stained with an aqueous, saturated solution of uranyl acetate and lead citrate (Reynolds 1963). The ultrathin sections were examined with a JEOL JEM-100S transmission electron microscope operated 60 kV.

Scanning electron microscopy and photomacrography

The gills for scanning electron-microscopy were fixed in phosphate-buffered glutaraldehyde (see above) for 45–60 min at ambient temperature and washed with 0.1 M Millonig's phosphate buffer (pH 7.4). The gills were individually photographed with a single-lens reflex camera equipped with a bellows and wide-field lens and then slowly dehydrated in graded solutions of ethanol. After several changes of absolute ethanol, the specimens were dried in a Bomar SPC-900/EX critical-point apparatus, with carbon dioxide as the transitional fluid. Dried specimens were secured to aluminum stubs with double-sided cellophane tape or silver paint and coated with a gold-palladium film (approximately 25 nm in thickness) in a Technics (Anatech) Hummer V sputtering system. They were examined with a JEOL JSM-35CF scanning electron microscope operated at 10 kV.

Results

The decapod crustacean *Carcinus maenas* possesses nine pairs of phyllobranchiate gills. Gills of the first pair are the shortest (approximately 4 mm in length), and those of the sixth pair are the longest (approximately 20 mm in length). Gills of the seventh, eighth, and ninth pairs exhibit the highest activities of Na^+/K^+-ATPase (Siebers et al. 1982), an enzyme that mediates ionic exchanges across cellular membranes (Neufeld et al. 1980). The gills consist of paired serial plates or lamellae along a raphe (central stem). The lamellae decrease in size distally (Figs. 1, 2). Bulbous knobs and ridges at the edges of the plates ensure the patency of the interlamellar spaces (Figs. 2, 4).

Typical lamellae are illustrated in Fig. 3. The plates are alar in shape and connected medially to the raphe which joins the incurrent (afferent) and excurrent (efferent) hemolymph channels. Cuspidate projections arise from mamillate mounds (Fig. 5) situated along the outer surface of the excurrent channel (Fig. 1). The functional significance of these structures, tentatively called gill spines, is not known. Bundles of neurites and true blood vessels do occur close by, suggesting the possibility that the spines have a sensory role (M.J. Cavey, S.H. Goodman, and E.C. Yeung, unpublished observations). Gill lamellae are limited by a chitinous, multilayered cuticle (Figs. 6, 7). The cuticle consists of three zones: an inner endocuticle that is approximately 0.8 μm thick, a middle exocuticle that is approximately 1.2 μm thick, and an outer epicuticle that is slightly less than 0.1 μm thick (Fig. 11). Energy-dispersive x-ray spectrometry indicates that the electron-dense granules at the interface of the endocuticle and exocuticle contain calcium or iron (M.J. Cavey, S.H. Goodman, and G.H. Curtis, unpublished observations). The epicuticular surfaces of the gill plates are largely obscured by two populations of adherent bacteria (Figs. 7, 8). Spectrometric analyses also reveal the presence of iron within the bacterial layer, endorsing the view that iron enters the cuticle from the branchial cavity (Johnson 1980) and possibly explaining the histochemical observation of iron-coated gill plates (Martin and Odense 1974).

The apical surface of the branchial epithelium adjoins the undersurface of the endocuticle. The intralamellar hemocoel (Figs. 6–9) is crossed by epithelial projections (Fig. 8), and perforated cellular shelves are often located equidistant from the proximal and distal surfaces of the lamellae (Fig. 6). These shelves, called lamellar septa (Barra et al. 1983), can occupy considerable space (Fig. 17). A filamentous basal lamina lies beneath the adcuticular epithelium and over the lamellar septa, thus marking the limits of the hemocoel (Fig. 9).

Five cell types can be identified within the branchial epithelium: the chief cell, the pillar cell (Drach 1930; "pilaster cell": Copeland 1968, Copeland and Fitzjarrell 1968), the striated cell ("salt-absorbing cell": Copeland and Fitzjarrell 1968; "salt-transporting cell": Barra et al. 1983), the nephrocyte (Cuénot 1893; "branchial podocyte": Johnson 1980), and the glycocyte (Fig. 27). The apical surfaces of the chief cells, pillar cells, and

Fig. 1. Photomacrograph of a gill from the seventh pair. The proximal end of the gill appears in the lower left corner of the field. A row of gill spines (*arrowheads*) appears over the excurrent hemolymph channel (*ex*). ×4; *bar:* 1 mm. **Fig. 2.** Scanning electron micrograph of the distal end of a gill from the seventh pair. Peripheral dilations ensure separation of the facing surfaces of adjoining lamellae; *ex* excurrent hemolymph channel. ×40; *bar:* 500 μm. **Fig. 3.** Montage of scanning electron micrographs of two pairs of gill lamellae and their relationships to the incurrent (*in*) and excurrent (*ex*) hemolymph channels. ×20; *bar:* 1 mm. **Fig. 4.** Scanning electron micrograph of three cross-fractured gill lamellae showing their peripheral dilations; *c* cuticle. ×220; *Bar:* 100 μm. **Fig. 5.** Scanning electron micrograph of a gill spine situated over the excurrent hemolymph channel. ×180; *bar:* 100 μm

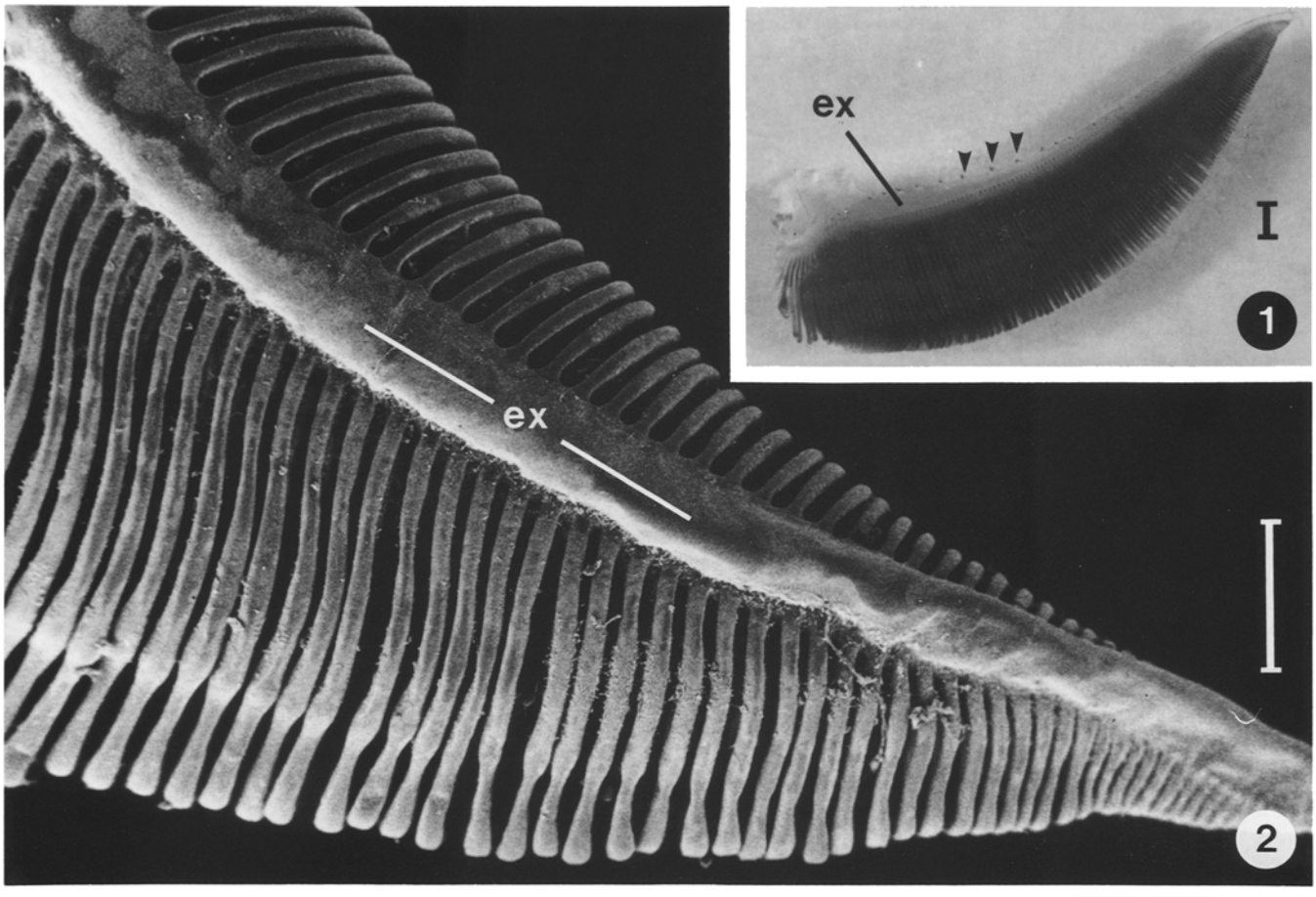

1

2

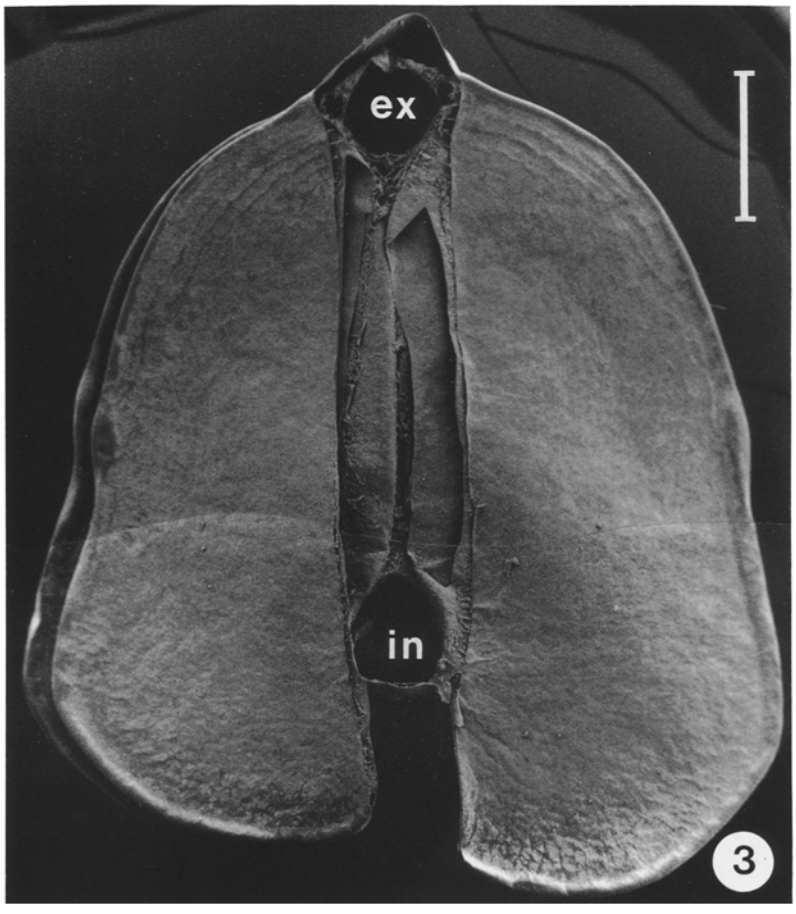

3

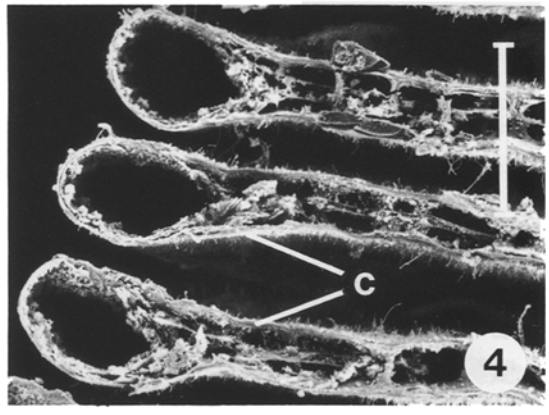

4

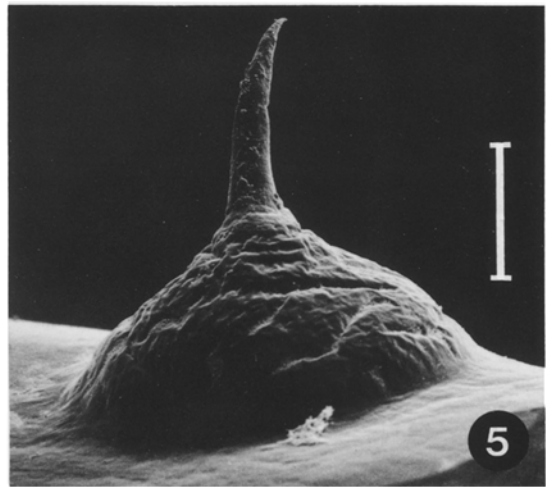

5

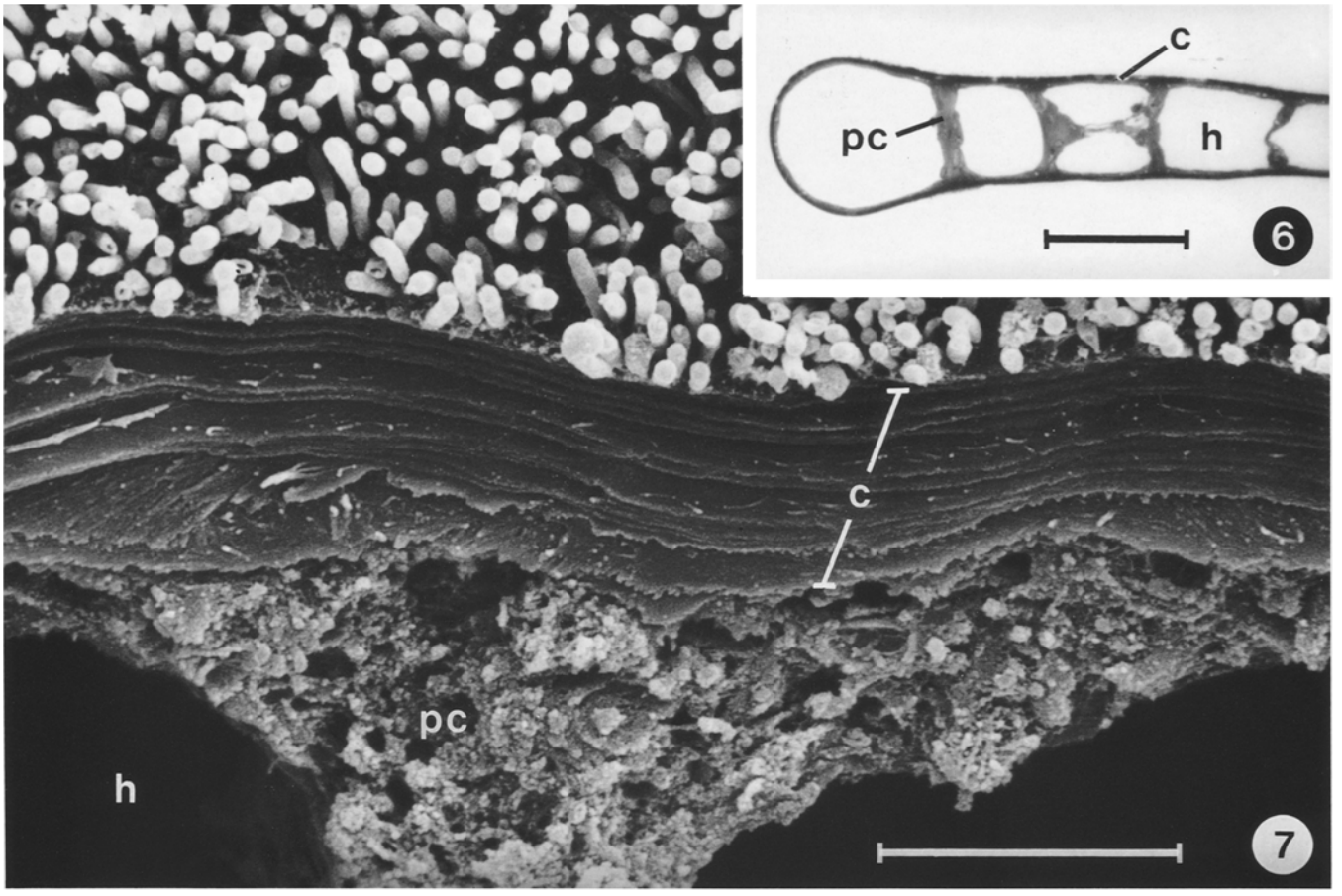
c
pc
h
6
c
pc
h
7

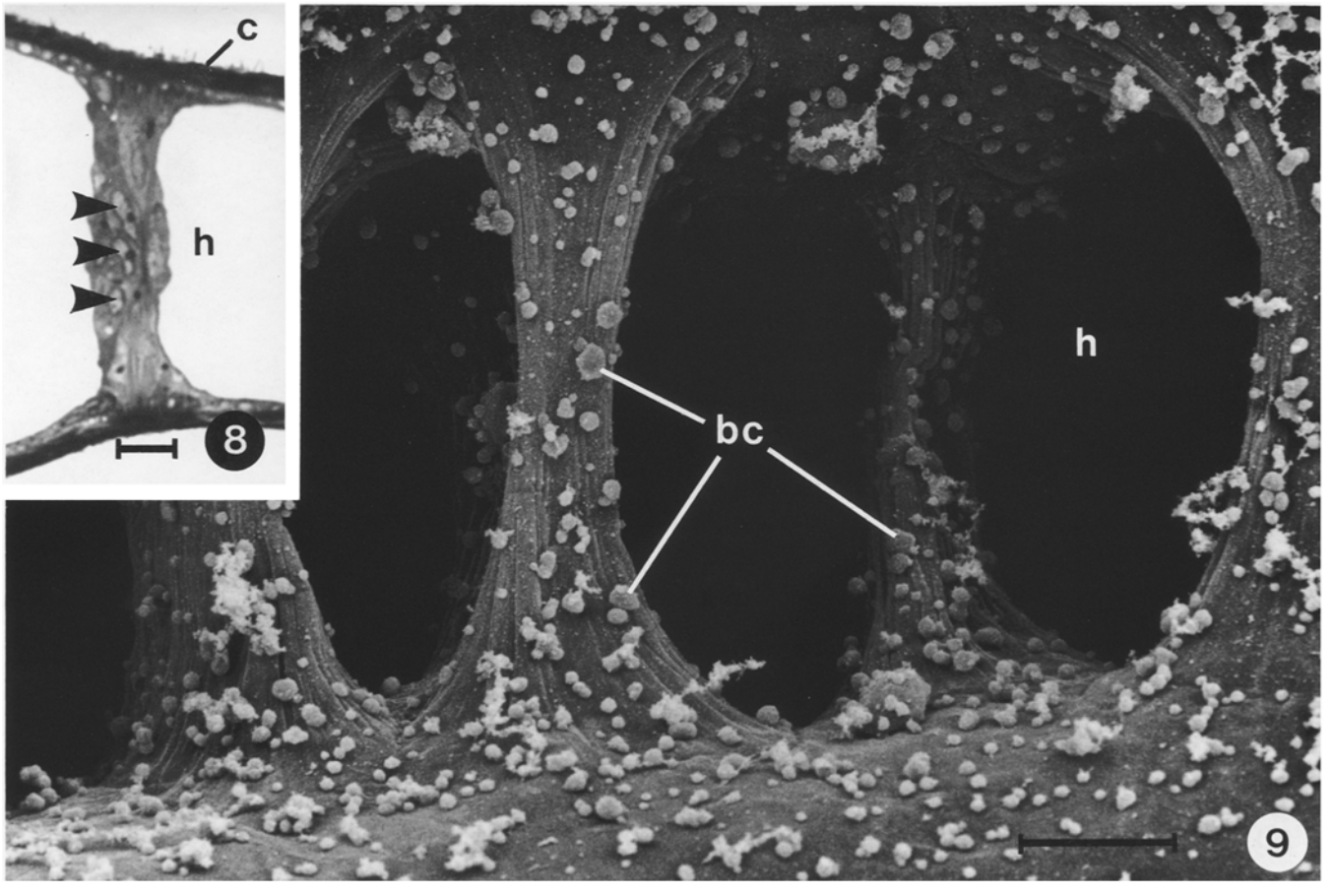
c
h
8
h
bc
9

striated cells adjoin the endocuticle. The nephrocytes and glycocytes do not contact the cuticle, but affiliation with the branchial epithelium is confirmed by their participation in intercellular junctions and by their position internal to the basal lamina.

The stems of pillar cells project across the hemocoel (Fig. 6), linking the proximal and distal sectors of the branchial epithelium. Cellular stems seldom span the hemocoel alone. Instead, several stems converge and traverse the hemocoel together as a multicellular stalk. Thin sections can reveal the presence of several nuclei within the pillar stalks (Fig. 8), and the cytoplasmic boundaries of the individual stems are clearly resolved in ultrathin sections (Fig. 14). The epithelial basal lamina completely surrounds each pillar stalk (Figs. 9, 10, 13).

The apical plasmalemmal segments of the pillar cells are folded (Figs. 10, 12), and the incisures contain an electron-dense, amorphous substance that resembles the chitinous material in the adjoining endocuticle. The broad folds of the plasma membranes obviously amplify the surface areas of the pillar cells and probably bolster the epithelial attachment to the cuticle. Besides the apical incisures, the pillar cells are distinguished by large bundles of cytoplasmic microtubules. The microtubules are ubiquitous organelles (Fig. 10). They lie parallel to the apical plasmalemmal folds and converge to enter the cellular stems that form the pillar stalks (Fig. 14). Were it not for the prevalence of microtubules, the attenuated regions of the pillar cells would be very difficult to distinguish from the squamous (chief and striated) cells. The lateral surfaces of the pillar cells, chief cells, and striated cells are affixed by junctional complexes with apical desmosomes and subapical septate junctions (Fig. 15). Putative gap junctions, appearing as macular appositions of the plasmalemmata, are occasionally found below the level of the septate junctions.

The squamous cells account for the majority of the epithelial surface area applied to the cuticle. The chief cells are the predominant cells, and in many gill plates the branchial epithelium consists almost entirely of this cell type (Fig. 6). Chief cells range in height from 2 μm to 5 μm, with the shorter cells confined to plates without lamellar septa. Blood cells in the hemocoel closely approach the chief cells (Fig. 18). The chief cells show numerous mitochondria and large, irregularly shaped vacuoles (Fig. 16). The membranes of the apices of the chief cells are infolded. Plasmalemmal invaginations are quite narrow, and they follow straight or arcuate courses into the cytoplasm (Fig. 16). Chief cells lining the "marginal canals" (Barra et al. 1983) in the peripheral dilations of the gill plates become extremely thin and electron-dense (Fig. 17). The height of such cells is about 0.5 μm, which is less than the thickness of the overlying cuticle (Fig. 20).

Striated cells are usually confined to gill plates with lamellar septa (Fig. 19) and then restricted to areas near the excurrent hemolymph channel and close to the raphe. The striated cells are approximately 5.5 μm in height and display modest systems of apical plasmalemmal folds and prominent networks of basal folds. Basal folds penetrate deep into the cytoplasm, and a single mitochondrion typically appears within each fold (Fig. 21). The folds of neighboring cells interdigitate freely. We have not identified intercellular junctions between the folds, although they have been reported between the folds of comparable cells in other crustaceans (Nakao 1974; Finol and Croghan 1983).

Nephrocytes are encountered in both the gill plates and the raphe. In the gill plates, they occur near the pillar stalks and, if present, the lamellar septa (Fig. 17). The clusters of nephrocytes often include glycocytes (Fig. 22). Glycocytes preferentially reside in those plates with lamellar septa.

The nephrocytes are large, subspherical cells with diameters in excess of 20 μm (Fig. 23). The nucleus, displaced to the periphery of the cell, is dwarfed by a massive central vacuole containing a heterogeneous, electron-dense substance. Several satellite vacuoles with similar contents flank the central vacuole. The Golgi apparatus is well developed in the nephrocyte, but the most striking cellular feature is a rim of foot processes or pedicels (Fig. 24), created by the interdigitation of branched cytoplasmic processes. The outer plasmalemmal leaflets of adjoining pedicels are joined by thin, electron-dense diaphragms. Pits are prevalent in plasmalemmal sectors behind the diaphragms, and small vesicles, carrying flocculent material similar to that immediately outside the cell, populate the cortical cytoplasm. Where a nephrocyte comes into close proximity of other epithelial cells, its pedicels give way to desmosomes. The basal lamina is excluded from these sites of cellular anchorage (Fig. 26).

Glycocytes assume various shapes. The nucleus of a glycocyte occupies a central position, and the cytoplasm is packed with glycogen granules and multigranular rosettes. The perinuclear cytoplasm is devoid of glycogen granules, creating a pale zone occupied by short cisternae of the endoplasmic reticulum and a few diminutive mitochondria (Fig. 25). Glycocytes, like nephrocytes, can form desmosomes with the other members of the branchial epithelium.

Discussion

The crab *Carcinus maenas* is a popular model system in physiological studies of the branchial epithelium. Histology and ultrastructure of the gills have until now been better appreciated in other crabs, such as *Eriocheir sinensis* (Barra et al. 1983; Gilles and Péqueux 1985), *Gecar-*

Fig. 6. Photomicrograph of a gill lamella revealing the cuticle (*c*), a branchial epithelium with pillar cells (*pc*), and the hemocoel (*h*). A lamellar septum spans between two of the pillar stalks. ×370; *bar:* 50 μm. **Fig. 7.** Scanning electron micrograph of a fractured pillar cell (*pc*). Observe the laminae of the cuticle (*c*) and the bacteria adhering to the epicuticle; *h* hemocoel. ×7650; *bar:* 5 μm. **Fig. 8.** Photomicrograph of a gill lamella showing the nuclei (*arrowheads*) of several pillar cells spanning the hemocoel (*h*); *c* cuticle. ×625; *bar:* 10 μm. **Fig. 9.** Scanning electron micrograph of pillar stalks traversing the hemocoel (*h*). Blood cells (*bc*) adhere to the basal lamina of the branchial epithelium. ×2000; *bar:* 10 μm

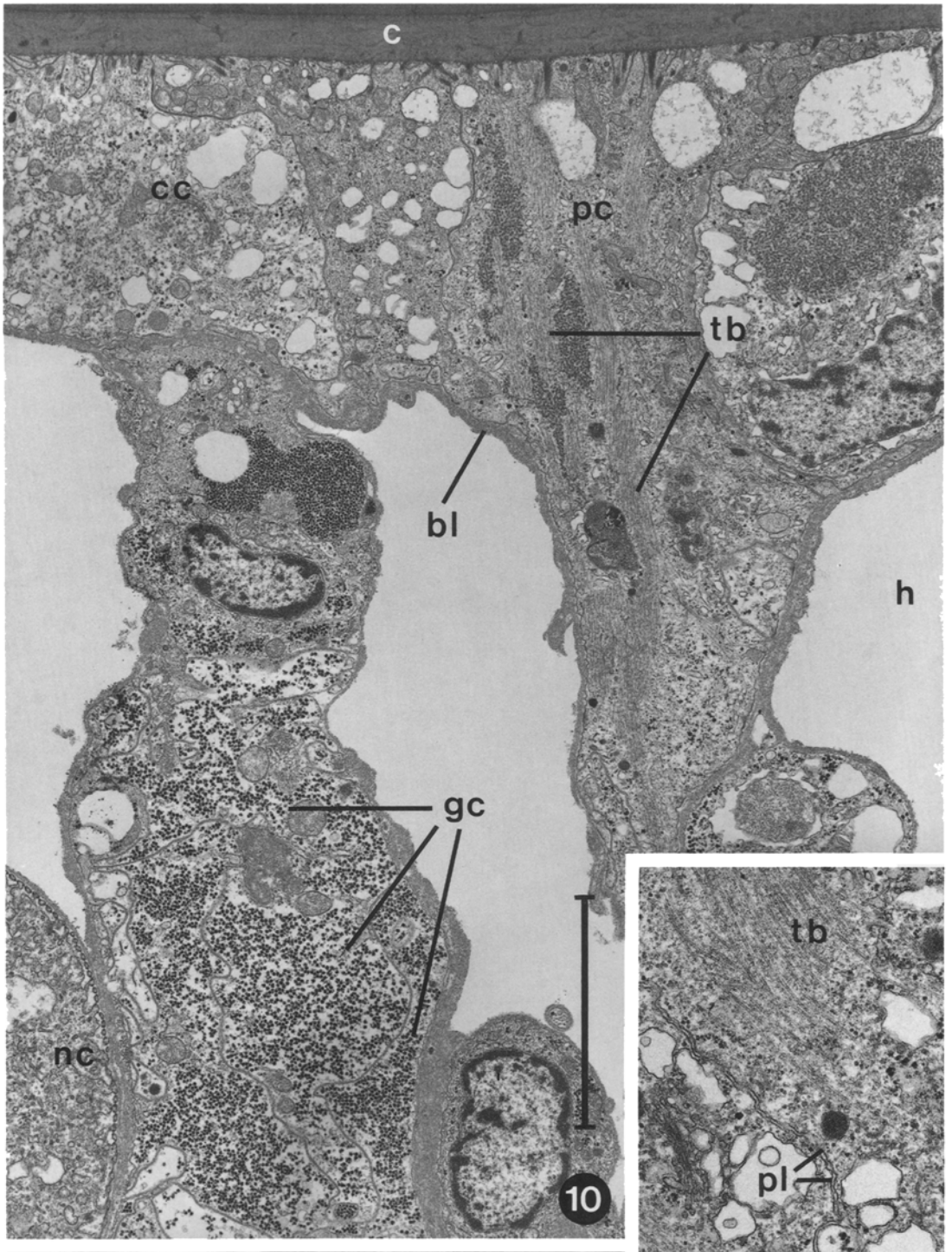
c
cc
pc
tb
bl
h
gc
nc
10

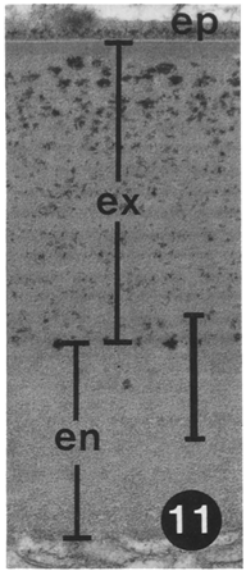
ep
ex
en
11

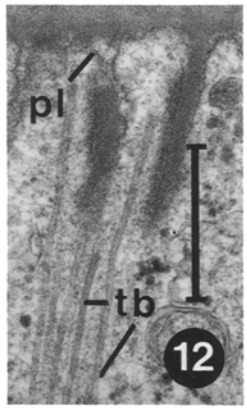
pl
tb
12

tb
pl
tb
14

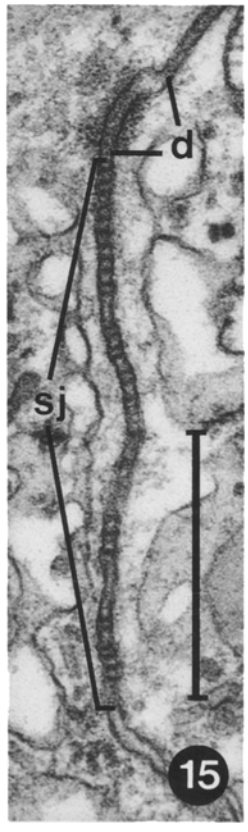
d
sj
15

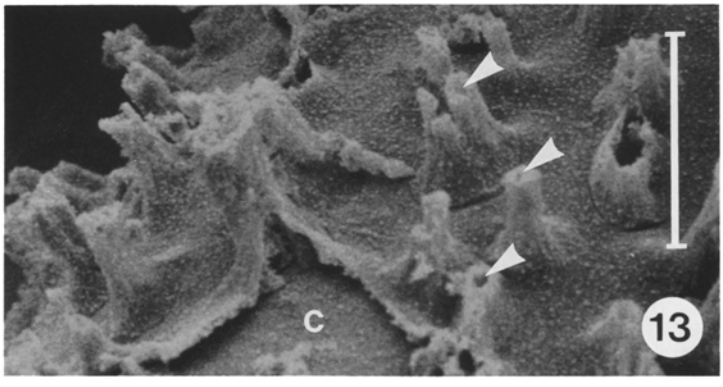
c
13

cinus lateralis (Copeland 1968), *Callinectes sapidus* (Copeland and Fitzjarrell 1968; Johnson 1980; Cioffi 1984), and *Uca mordax* (Finol and Croghan 1983).

Lamellae are densely packed in the phyllobranchiate gills of *C. maenas*. This organizational pattern should maximize the surface area for respiration and ionoregulation, and peripheral dilations of the gill plates ensure the patency of interlamellar spaces. The discovery of gill spines over the excurrent hemolymph channels was unexpected. Similar structures have not been reported in the gills of closely related species. Nerves have not been found previously in the gills of *C. maenas*, although they have been described in the gills of the shrimp *Penaeus aztecus* (Foster and Howse 1978).

Morphological differences between the anterior and posterior gills of crabs have long been recognized and correlated with functional differences. The anterior gills generally serve respiratory functions, and the posterior ones bear the ionoregulatory tissue (Copeland 1968; Barra et al. 1983; Gilles and Péqueux 1985). In our study, we opted to examine the gills of the seventh pair which have the "thick" epithelial regions associated with ionoregulation and the "thin" epithelial sectors related to respiration (Towle and Kays 1986). We have observed that some lamellae are specialized only for respiration and others for both respiration and ionoregulation. The branchial epithelium of the former consists of chief cells and pillar cells, and the epithelium of the latter is an admixture of striated cells, chief cells, and pillar cells. Nephrocytes and glycocytes tend to localize in the epithelia of ionoregulatory lamellae.

The pillar cells probably include the "trabecular cells" described by Nakao (1974) in the lamellar septa. The contributions of multiple cells to formation of a single pillar have been noted previously. Johnson (1980) proposed that pillars consist of two cells from opposite sides of a lamella that meet in the middle of the hemocoel. In *C. maenas*, as in *E. sinensis* (Barra et al. 1983), this is clearly not the case. The stems of several cells occur in each pillar, and the stems are likely intertwined in a spiral fashion. Pillar stalks conceivably maintain the patency and uniform width of the hemocoel (Cioffi 1984), and the prevalence of microtubules within the cells is certainly consonant with such proposals (Fisher 1972; Finol and Croghan 1983; Martelo and Zanders 1986).

The striated cells of *C. maenas* meet the morphological parameters ascribed to ionoregulatory cells in crustaceans, other invertebrates, and vertebrates (Barra et al. 1983; Talbot et al. 1972). The cells exhibit infolding of the apical plasmalemmata and extensive basal folding. The degree of apical cellular folding in *C. maenas* is considerably less than illustrated in *E. sinensis* (Barra et al. 1983) and *C. sapidus* (Copeland and Fitzjarrell 1968; Johnson 1980). We might rationalize this anomaly by noting that our animals were acclimated to normal sea water and, thus, not subjected to an osmotically stressful environment. Gilles and Péqueux (1985) believe that cells forfeit the ability to pump ions in sea-water-acclimated crabs. They contend that ionic pumping gradually returns as animals acclimate to fresh water and that resumption of this activity is manifest in the lengthening of the apical cellular folds. A direct relationship between osmotic stress and cellular appearance may

Fig. 10. Transmission electron micrograph showing general features of the branchial epithelium. The apical epithelial surface adjoins the cuticle (*c*), and a basal lamina (*bl*) segregates the epithelium from the hemocoel (*h*). A pillar cell (*pc*), a chief cell (*cc*), a nephrocyte (*nc*), and several glycocytes (*gc*) are illustrated; *tb* microtubules. ×7100; *bar:* 5 μm. **Fig. 11.** Transmission electron micrograph of the tripartite cuticle (*ep* epicuticle; *ex* exocuticle; *en* endocuticle). ×32200; *bar:* 0.5 μm. **Fig. 12.** Transmission electron micrograph of the apical incisures of a pillar cell. The endocuticle is directly continuous with the electron-dense material in the incisures; *pl* plasmalemma; *tb* microtubule. ×38000; *bar:* 0.5 μm. **Fig. 13.** Scanning electron micrograph of cleaved pillar stalks. The stalks occasionally appear hollow (*arrowheads*). The cuticle (*c*) of the gill lamella is visible through a tear in the branchial epithelium. ×540; *bar:* 50 μm. **Fig. 14.** Transmission electron micrograph of the bundles of microtubules (*tb*) in pillar cells of the branchial epithelium; *pl* plasmalemma. ×18600; *bar:* 1 μm. **Fig. 15.** Transmission electron micrograph of a junctional complex between branchial epithelial cells. Limits of the desmosome (*d*) and the underlying septate junction (*sj*) are indicated. ×72200; *bar:* 0.5 μm

Fig. 16. Transmission electron micrograph of chief cells. Apical sectors of the plasmalemma are invaginated (*white arrowheads*), and the basal interdigitation of cells and cellular processes (*black arrowheads*) is also apparent; *bl* basal lamina; *c* cuticle; *jc* junctional complex. ×11300; *bar:* 1 μm. **Fig. 17.** Photomicrograph of a lamellar septum (*arrowhead*) within a gill plate. Nephrocytes (*nc*), glycocytes (*gc*), and a zone of extremely thin chief cells (*cc*) are evident; *h* hemocoel. ×230; *bar:* 100 μm. **Fig. 18.** Transmission electron micrograph of chief cells and a blood cell (*bc*) in the adjoining hemocoel (*h*). Blood cells conceivably utilize the basal lamina (*bl*) of the branchial epithelium as a substratum for attachment and/or movement; *c* cuticle. ×11400; *bar:* 1 μm. **Fig. 19.** Photomicrograph of striated cells (*sc*), pillar cells (*pc*), and nephrocytes (*nc*); *h* hemocoel. ×390; *bar:* 10 μm. **Fig. 20.** Transmission electron micrograph of a lamellar dilation with extremely thin, electron-dense chief cells (*cc*). Cytoplasmic density interferes with the examination of cytoplasmic organelles and inclusions; *bl* basal lamina; *c* cuticle. ×27600; *bar:* 1 μm. **Fig. 21.** Transmission electron micrograph of striated cells. The cells are basally folded (*arrowheads*) and interdigitated. Mitochondria align within the deep basal folds; *bl* basal lamina; *jc* junctional complex. ×13500; *bar:* 1 μm

Fig. 22. Photomicrograph of a cluster of nephrocytes (*nc*) and dispersed glycocytes (*gc*) within a gill lamella. The massive central vacuoles of the nephrocytes stain intensely; *pc* pillar cell. ×470; *bar:* 10 μm. **Fig. 23.** Transmission electron micrograph of a nephrocyte. Satellite vacuoles (*arrowheads*) flank the massive central vacuole. Pedicels project toward the enveloping basal lamina (*bl*) ×8400; *bar:* 1 μm. **Fig. 24.** Transmission electron micrograph of the pedicels of a nephrocyte. Diaphragms (*arrowheads*) between the pedicels are distinctly thinner than the cellular membrane; *bl* basal lamina. ×22200; *bar:* 0.5 μm. **Fig. 25.** Transmission electron micrograph of pleomorphic glycocytes with glycogen granules and multigranular rosettes (*gly*). ×13300; *bar:* 1 μm. **Fig. 26.** Transmission electron micrograph of the apposition of a nephrocyte (*nc*) and several glycocytes (*gc*). The cells are anchored by desmosomes (*d*). The basal lamina (*bl*) of the branchial epithelium penetrates between the cells but is excluded from the junctional domains. ×16600; *bar:* 1 μm

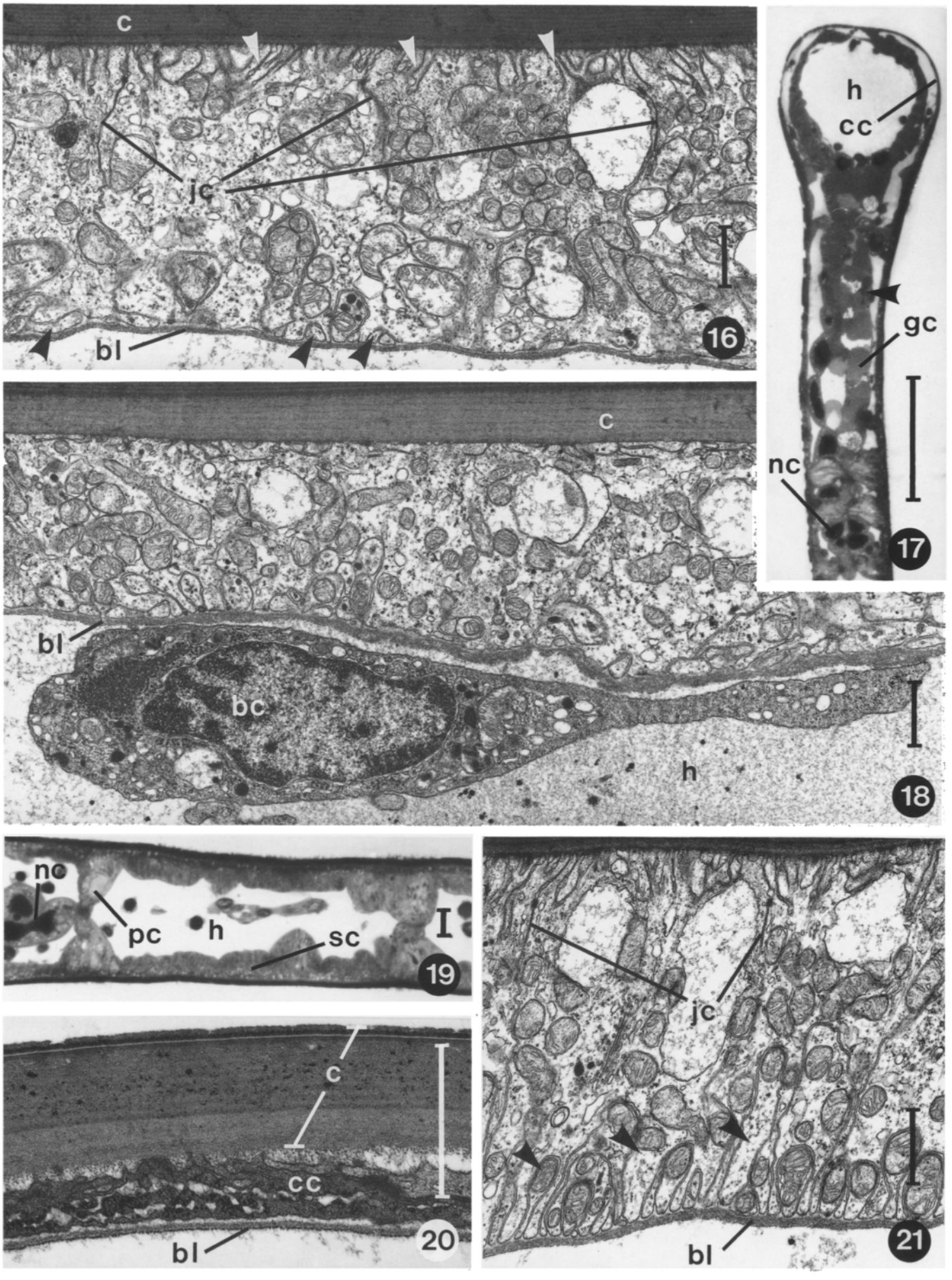

Figs. 16–21

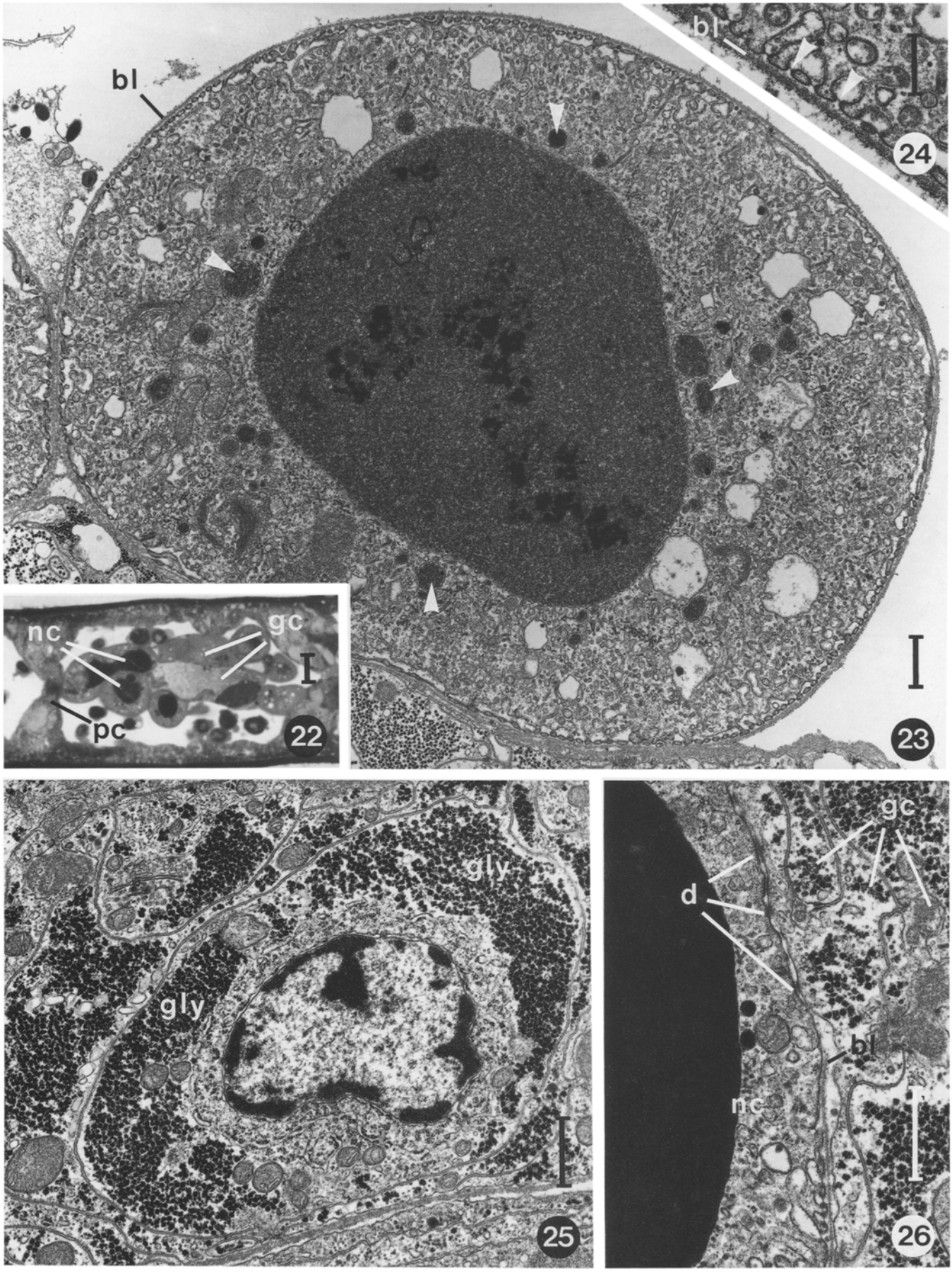

Figs. 22–26

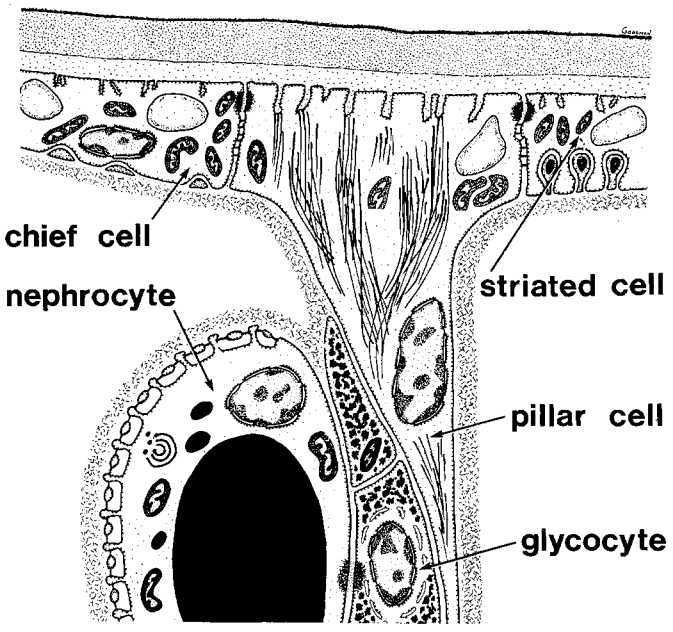

Fig. 27. Schematic diagram of the five constituent cells of the branchial epithelium of *Carcinus maenas*. Salient cytoplasmic features are illustrated. Ultrastructural features have been simplified or exaggerated in size to better illustrate relationships of the cells to the cuticle of the gill lamella, the intralamellar hemocoel, the epithelial basal lamina, and each other

not hold universally. Elaborate cellular folds persist in *Goniopsis cruentata* even after acclimation to sea water (Martelo and Zanders 1986).

The basal folds of the striated cells interdigitate with those from neighboring cells. Mitochondria aggregate within the deep basal folds, giving rise to the so-called "mitochondrial pump", which some investigators equate with salt transport (Copeland 1967, 1968; Copeland and Fitzjarrell 1968). Others dispute this assumption, contenting that mitochondrial aggregation is an inevitable consequence of accommodating abundant organelles into confined cytoplasmic spaces (Finol and Croghan 1983).

Barra et al. (1983) hypothesize that intralamellar septa determine the flow pattern of hemolymph within the gill plate and serve as storage depots for glycogen. Septa are found in only some gill plates of *C. maenas*, so it is difficult to believe that determination of the pattern of hemolymph flow is a major function. We do, however, consistently find glycocytes near the septa in ionoregulatory lamellae. It might prove informative to investigate the possibility of a functional link between the striated cells and glycocytes.

The nephrocytes of *C. maenas* are undistinguished from those already described in the gills of other crustaceans (Wright 1964; Morse et al. 1970; Strangways-Dixon and Smith 1970; Doughtie and Rao 1978; Foster and Howse 1978; Johnson 1980). Their membership in the branchial epithelium is easily justified, when one recognizes their position relative to the epithelial basal lamina and their ability to form intercellular junctions (Strangways-Dixon and Smith 1970; Foster and Howse 1978). Ultrastructurally, the nephrocytes superficially resemble the podocytes of vertebrates and, as in the kidney, the epithelial basal lamina and the diaphragms between pedicels have been proposed as filtration devices (Strangways-Dixon and Smith 1970). From a functional standpoint, however, it seems more appropriate to analogize the branchial nephrocytes to the fixed macrophages of vertebrate sinusoids. The nephrocytes are suitably positioned to endocytose toxic and/or foreign elements from the hemolymph. Following the action of lysosomal enzymes on the membrane-bounded materials, the cells could exocytose inert substances back to the hemolymph.

With this morphological survey at hand, we can now consider the alterations of the branchial epithelium of *C. maenas* in response to osmotic stress. Changes to the striated cells, namely the amplification of apical and/or basal folds, have been observed in many (Lockwood et al. 1973; Milne and Ellis 1973; Foster and Howse 1978; Gilles and Péqueux 1985) but not all (Bubel 1976; Finol and Croghan 1983) crustacean gills examined thus far. Before proceeding, however, we must unequivocally determine which gills are specialized for ionoregulation and which sectors of their lamellae are participants. Our initial attempts to map the ionoregulatory regions with the silver nitrate technique (Koch 1934) have failed, owing to the interference of the adherent bacteria. In a companion paper, we shall illustrate this bacterial interference and also show how the bacteria segregate on the epicuticle in patterns that relate to the organization of the underlying branchial epithelium.

Acknowledgements. This project was supported by Research Operating Grant No. A0484 from the Natural Sciences and Engineering Research Council of Canada.

References

Barra JA, Péqueux A, Humbert W (1983) A morphological study on gills of a crab acclimated to fresh water. Tissue Cell 15:583–596

Bubel A (1976) Histological and electron microscopical observations on the effects of different salinities and heavy metal ions, on the gills of *Jaera nordmanni* (Rathke) (Crustacea, Isopoda). Cell Tissue Res 167:65–95

Cavey MJ, Curtis GH (1987) Morphology of the phyllobranchiate gills of a euryhaline crab. Am Zoologist 27:151A

Cioffi M (1984) Comparative ultrastructure of arthropod transporting epithelia. Am Zoologist 24:139–156

Cloney RA, Florey E (1968) Ultrastructure of cephalopod chromatophore organs. Z Zellforsch 89:250–280

Copeland DE (1967) A study of salt secreting cells in the brine shrimp (*Artemia salina*). Protoplasma 63:363–384

Copeland DE (1968) Fine structure of salt and water uptake in the land-crab, *Gecarcinus lateralis*. Am Zoologist 8:417–432

Copeland DE, Fitzjarrell AT (1968) The salt absorbing cells in the gills of the blue crab (*Callinectes sapidus* Rathbun) with notes on modified mitochondria. Z Zellforsch 92:1–22

Cuénot L (1893) Etudes physiologiques sur les Crustacés décapodes. Arch Biol Lieges 13:245–303

Doughtie DG, Rao KR (1978) Ultrastructural changes induced by sodium pentachlorophenate in the grass shrimp, *Palaemon-*

etes pugio, in relation to the molt cycle. In: Rao KR (ed) Pentachlorophenol, Chemistry, pharmacology, and environmental toxicology. Plenum Press, New York London, pp 213–250

Drach P (1930) Etude sur le système branchial des Crustacés décapodes. Arch Anat Microsc 26:83–133

Finol HJ, Croghan PC (1983) Ultrastructure of the branchial epithelium of an amphibious brackish-water crab. Tissue Cell 15:63–75

Fisher JM (1972) Fine-structural observations on the gill filaments of the fresh-water crayfish, *Astacus pallipes* Lereboullet. Tissue Cell 4:287–299

Foster CA, Howse HD (1978) A morphological study on gills of the brown shrimp, *Penaeus aztecus*. Tissue Cell 10:77–92

Gilles R, Péqueux AJR (1985) Ion transport in crustacean gills: Physiological and ultrastructural approaches. In: Gilles R, Gilles-Baillien M (eds) Transport processes, iono- and osmoregulation. Springer, Berlin Heidelberg New York, pp 138–158

Goodman SH, Cavey MJ (1988) Epithelial cells in the phyllobranchiate gills of the shore crab. Am Zoologist 28:142A

Johnson PT (1980) Histology of the blue crab, *Callinectes sapidus*. A model for the Decapoda. Praeger Publishers, New York, pp 84–100

Koch H (1934) Essai d'interprétation de la soi-disant «réduction vitale» de sels d'Argent par certains organes d'Arthropodes. Ann Soc Sci Med Nat Bruxelles 54B:346–361

Lockwood APM, Inman CBE, Courtenay TH (1973) The influence of environmental salinity on the water fluxes of the amphipod crustacean *Gammarus duebeni*. J Exp Biol 58:137–148

Luft JH (1961) Improvements in epoxy resin embedding methods. J Biophys Biochem Cytol 9:409–414

Martelo M-J, Zanders IP (1986) Modifications of gill ultrastructure and ionic composition in the crab *Goniopsis cruentata* acclimated to various salinities. Comp Biochem Physiol 84A:383–389

Martin J-LM, Odense PH (1974) Le fer dans la branchie des Crustacés décapodes *Carcinus maenas* (L.) et *Homarus americanus* Milne Edw.: Étude quantitative et histochimique. J Exp Mar Biol Ecol 16:123–130

Milne DJ, Ellis RA (1973) The effect of salinity acclimation on the ultrastructure of the gills of *Gammarus oceanicus* (Segerstråle, 1947) (Crustacea: Amphipoda). Z Zellforsch 139:311–318

Morse HC, Harris PJ, Dornfeld EJ (1970) *Pacifastacus leniusculus:* fine structure of arthrobranch with reference to active ion uptake. Trans Am Microsc Soc 89:12–27

Nakao T (1974) Electron microscopic study of the open circulatory system of the shrimp, *Caridina japonica*. I. Gill capillaries. J Morphol 144:361–380

Neufeld GJ, Holliday CW, Pritchard JB (1980) Salinity adaption of gill Na, K-ATPase in the blue crab, *Callinectes sapidus*. J Exp Zool 211:215–224

Reynolds ES (1963) The use of lead citrate at high pH as an electron-opaque stain in electron microscopy. J Cell Biol 17:208–212

Richardson KC, Jarett L, Finke EH (1960) Embedding in epoxy resins for ultrathin sectioning in electron microscopy. Stain Technol 35:313–323

Siebers D, Leweck K, Markus H, Winkler A (1982) Sodium regulation in the shore crab *Carcinus maenas* as related to ambient salinity. Mar Biol 69:37–43

Strangways-Dixon J, Smith DS (1970) The fine structure of gill 'podocytes' in *Panulirus argus* (Crustacea). Tissue Cell 2:611–624

Talbot P, Clark Jr WH, Lawrence AL (1972) Light and electron microscopic studies on osmoregulatory tissue in the developing brown shrimp, *Penaeus aztecus*. Tissue Cell 4:271–286

Towle DW, Kays WT (1986) Basolateral localization of $Na^+ + K^+$-ATPase in gill epithelium of two osmoregulating crabs, *Callinectes sapidus* and *Carcinus maenas*. J Exp Zool 239:311–318

Wood RL, Luft JH (1965) The influence of buffer systems on fixation with osmium tetroxide. J Ultrastruct Res 12:22–45

Wright KA (1964) The fine structure of the nephrocyte of the gills of two marine decapods. J Ultrastruct Res 10:1–13

Zatta P, Milanesi C (1984) Ultrastruttura delle branchie di *Carcinus maenas*. Boll Soc Ital Biol Sper 60:1385–1391